Differential Brillouin gain for improving the temperature accuracy and spatial resolution in a long-distance distributed fiber sensor

Yongkang Dong, Xiaoyi Bao,* and Wenhai Li

Fiber Optical Group, Department of Physics, University of Ottawa, 150 Louis Pasteur, Ottawa, Ontario K1N 6N5, Canada

*Corresponding author: xbao@uottawa.ca

Received 4 May 2009; accepted 24 June 2009;
posted 6 July 2009 (Doc. ID 110887); published 21 July 2009

We demonstrate a 12 km differential pulse-width pair Brillouin optical time-domain analysis (DPP-BOTDA) using 40 ns and 50 ns pulses with DC-coupled detection. A spatial resolution of 1 m and a narrowband Brillouin gain spectrum of 33 MHz are obtained simultaneously compared with 88 MHz with the use of 10 ns pulses in a conventional BOTDA. The experimental results show that the differential Brillouin gain of a 40/50 ns pulse pair is 7 times stronger than the direct Brillouin gain of BOTDA with the use of a 10 ns pulse, and the temperature uncertainty is 0.25 °C compared with 1.8 °C for a 10 ns pulse. As the pulse-width difference decreases from 10 ns to 1 ns, corresponding to a spatial resolution from 1 m to 10 cm, the prediction of temperature uncertainty will only increase from 0.25 °C to 0.8 °C for DPP-BOTDA over a 12 km long single-mode fiber.

OCIS codes: 280.4788, 290.5900.

1. Introduction

Long-distance distributed Brillouin fiber sensors have attracted a great deal of interest due to their potential use for monitoring temperature and strain over large structures such as underground power cables, oil pipe lines, dams, and bridges. Several techniques have been proposed for effective sensing, and they can be classified into two types: Brillouin optical time-domain reflectometry (BOTDR) [1,2] and Brillouin optical time-domain analysis (BOTDA) [3,4]. BOTDR makes use of spontaneous Brillouin scattering from the probe pulse using only one end of the sensing fiber, while BOTDA is generally built up in loop configuration for the counterpropagating probe pulse and cw pump to induce stimulated Brillouin scattering (SBS).

However, for both cases there is a trade-off between the spatial resolution and the accuracy of the Brillouin frequency shift (BFS). The spatial resolution is determined by the pulse width, and it can be improved by using a short pulse; a short pulse will give a broadened Brillouin gain spectrum (BGS). The measured BGS is the convolution of the intrinsic SBS spectrum $g_{S0}(\nu_S)$ and the power spectrum of the pulsed light $P_p(\nu_p)$ and can be expressed as

$$g_S(\nu_S) = g_{S0}(\nu_S) \cdot P_p(\nu_p). \tag{1}$$

Considering a rectangular-shaped pulsed light, its power spectrum is given by

$$P_p(\nu_p) = P_0 \left[\frac{\sin \pi(\nu_p - \nu_0)\tau}{\pi(\nu_p - \nu_0)} \right]^2, \tag{2}$$

where ν_0 is the central frequency of the pulse, τ is the pulse width, and P_0 is a constant. Equation (2) shows that when τ is large enough (much larger than

0003-6935/09/224297-05$15.00/0

phonon lifetime of 10 ns in optical fiber), the light power is concentrated in a narrowband spectrum, so the measured BGS is almost the intrinsic SBS spectrum. In contrast, as τ becomes small, the light power is distributed over a wide frequency region, which results in broadened BGS. Furthermore, the shorter pulse width gives the weaker Brillouin signal and subsequently results in a smaller signal-to-noise ratio (SNR). These limitations prohibit one from obtaining a high spatial resolution and a high BFS accuracy simultaneously.

Recently, our group proposed a differential pulse-width pair Brillouin optical time-domain analysis (DPP-BOTDA) for high spatial resolution sensing [5]. This scheme employs two separate long pulses (a few tens of nanoseconds) with a small pulse-width difference (a few nanoseconds) to map the BGS of the sensing fiber. The differential BGS can be obtained by taking subtraction between the two BGSs, and its spatial resolution is determined by the pulse-width difference of the two separate long pulses. The DPP-BOTDA provides several advantages over conventional BOTDA: (1) Narrowband BGS (a few tens MHz) and high spatial resolution (smaller than 1 m) can be obtained simultaneously. (2) The differential BGS provides stronger signal intensity and thus better SNR than that of directly using the narrow pulse in BOTDA when the pulse-width difference of the two long pulses equals to the narrow pulse width.

In Ref. [5], an AC-coupled detection was used to record the time-domain Brillouin signal, which has the ability to extract very small change from a strong background. This method is preferable for a short-distance (usually smaller than 1 km) sensing fiber with high spatial resolution (sub meter level) using the probe pulse and cw pump power both in the magnitude of a few milliwatts [6]. For a long-distance sensing fiber (a few kilometers and larger), however, the Brillouin time-domain signals obviously decay because of the capacitor discharge of AC-coupled circuit, which limits the achievable longest length sensing fiber. In this paper, we use the DC-coupled detection to perform a 12 km DPP-BOTDA with a 40/50 ns pulse pair, and we study the differential Brillouin gain at various pulse-width differences comparing the signal level from direct Brillouin gain for a pulse width of 1–10 ns, which is equivalent to the spatial resolution of 10 cm to 1 m. With DPP-BOTDA for narrowband BGS of 33 MHz and considerable SNR improvement, we can always achieve temperature resolution better than 1 °C for the spatial resolution of 10 cm to 1 m.

2. Experimental Setup and Parameters

The DPP-BOTDA experimental setup is shown in Fig. 1. Two narrow linewidth (3 kHz) fiber lasers operating at 1550 nm were used to provide the probe and pump light, respectively, whose frequency difference was locked by a phase locking loop in a frequency counter and was automatically swept by

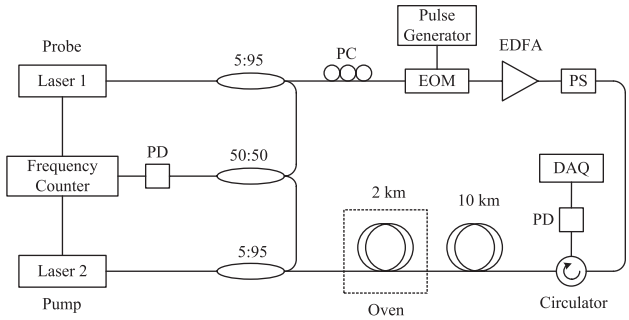

Fig. 1. Experimental setup for DPP-BOTDA: PD, photodetectors; PC, polarization controller; PS, polarization scrambler; EOM, electro-optic modulator; EDFA, erbium-doped fiber amplifier; DAQ, data acquisition.

varying the temperature of the fiber Bragg grating of the cavity controlled by a computer. A 12 GHz high-speed detector was used to measure the beat signal between the probe and the pump, which provided feedback to the frequency counter to lock the frequency. The probe laser was launched to a high extinction ratio electro-optic modulator (EOM) to create a probe pulse with an extinction ratio larger than 45 dB and then was amplified by an erbium-doped fiber amplifier (EDFA). A polarization scrambler was used to change the polarization state of the probe pulse continuously to reduce the polarization-mismatching-induced fluctuation of the signal by averaging a large number of signals. The Brillouin loss signal was detected by a DC-coupled photodetector with 1 GHz bandwidth. The sensing fiber comprises two segments, i.e., a segment of 10 km at ambient temperature and the other segment of 2 km in an oven.

In a conventional high-spatial-resolution distributed fiber sensor based on a Brillouin loss spectrum, a probe pulse and cw pump with a power of a few millwatts were used, and the change on the pump light induced by Brillouin loss is only one in a thousand or even smaller. AC-coupled detection was proposed to detect such a small change on a strong background, which has been proved successful in a high-spatial-resolution Brillouin sensor [6,7]. However, AC-coupled detection means blocking off the low-frequency information, which can be neglected for a short-distance sensing fiber. For a long-distance fiber sensor, the longer the fiber, the more low-frequency information is included in the signal. The Brillouin time-domain signals decay obviously in a long-distance sensing due to the AC-coupled circuit, which limits the achievable longest sensing distance. The usable sensing fiber length using AC-coupled detection is actually determined by the cutoff frequency of the low-frequency of the detector. A longer sensing length can be achieved by using a lower cutoff frequency of the low-frequency; however, a longer time is needed for the detector to recover from the charged state after the signal, which limits the probe pulse repetition, and consequently a longer time is needed to perform a measurement. Generally

speaking, a practical system using AC-coupled detection is suitable for short-distance application and usually is limited to a few hundred meters.

In our experiment, DC-coupled detection was used to perform a 12 km long-distance fiber sensor. Our system operates at 1550 nm, which falls in the gain bandwidth of the erbium-doped fiber amplifier. The peak power of the probe pulse was amplified to 300 mW to increase the Brillouin loss signal on the pump light. A small pump power of 0.3 mW was used to decrease the amplification to the probe pulse to avoid distorted BGS in the far end of the sensing fiber.

For the choice of the pulse-width pair in the DPP-BOTDA experiment, long pulses are preferable to obtain a narrow BGS; however, long pulses could saturate the direct Brillouin gain, resulting in a small differential gain. In our experiment, a pulse-width pair of 40 ns and 50 ns with a rising time of 2 ns was used as probe pulses, shown in Fig. 2, which provides the maximum differential gain and SNR under our experimental condition. Both pulses have the same leading edge and the same start point, which is the essential requirement for DPP-BOTDA. The differential pulse of this pulse pair is shown in the green line, which is the equivalent pulse for DPP-BOTDA actually determining the final spatial resolution and the start point of the differential Brillouin loss signal. In our experiment, the oven was heated to 60 °C, and the BFS of the heated 2 km fiber segment was around 10910 MHz. The 10 km fiber segment at ambient temperature had a BFS of around 10860 MHz.

3. Results and Discussion

The Brillouin loss signals of a 40/50 ns pulse pair and their differential signal at the transition region at the frequency difference of 10910 MHz are shown in Fig. 3(a). For the 40 ns pulse, the transition region starts from point a to point b covering 4 m, while it starts from point a to point c covering 5 m for the 50 ns pulse. The subtraction of the two Brillouin loss signals gives the differential signal shown as the green line, which starts from point b to point c covering 1 m. It is clear to see that, for the differential signal, the spatial resolution is equivalent to that of the differential pulse, and the start point of the signal is determined by the leading edge of the differential pulse.

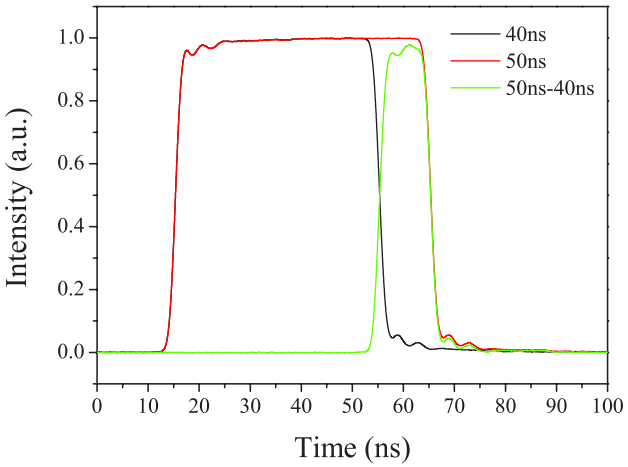

Fig. 2. (Color online) Time traces of 40 ns and 50 ns pulses and their differential pulse.

It can be seen that the Brillouin loss signals at the transition region for both two long pulses increase slowly during the first 10 ns and then enter into a linearly increasing regime. This is because about 10 ns is needed to establish the stimulated acoustic wave in the optical fiber, and just after the establishment of the acoustic wave the Brillouin gain increases linearly with the pulse width. As for the differential signal, it is attributed to the subtraction of the linearly increasing regime exhibiting large intensity compared with the increment in the initial establishing regime in the BOTDA case. Comparison of the direct gain signal of the first 10 ns and the differential gain signal of the last 10 ns is shown in Fig. 3(b). The direct gain signal and differential gain signal correspond to the signals of BOTDA and DPP-BOTDA, respectively. The direct gain signal experiences an exponential increasing at the acoustic wave establishing regime, while the differential signal exhibits a linearly increasing. The intensity improved ratio, defined as the ratio of the differential gain to the direct gain, is decreased with the time difference, showing a maximum value of 18.5 at 1 ns and a minimum value of 7 at 10 ns, as seen in Fig. 3(b).

The frequency difference of the probe and pump light was swept from 10800 MHz to 10968 MHz with a step of 4 MHz using 40 ns, 50 ns, and 10 ns probe pulses, respectively. The Brillouin loss signals were recorded at a 250 MHz/s sampling rate using 1000 averages. Due to the weak Brillouin loss signal for the 10 ns pulse, the cw pump power was increased to 0.7 mW to increase the SNR. The comparison of the measured BGSs of 10 ns pulse and 40/50 ns differential pulse pair is shown in Fig. 4 (in the fiber at a distance of 200 m). The Lorentzian fit of the differential BGS is shown in the red line with a bandwidth $\Delta\nu_B$ of 33 MHz and a standard deviation $\delta\nu_B$ of 0.3 MHz, which corresponds to a temperature uncertainty of 0.25 °C, while for direct use of a 10 ns pulse, its Lorentzian fit, shown as black line, has a $\Delta\nu_B$ of 88 MHz. The bandwidth and the SNR of the BGS determine the uncertainty of BFS [8],

$$\delta\nu_B = \Delta\nu_B/\sqrt{2}(\mathrm{SNR})^{1/4}. \quad (3)$$

Here the SNR refers to the electrical SNR. According to Fig. 3(b), compared with the direct gain signal, the optical SNR is improved by 7 times, with a 10 ns time difference for the differential gain signal corresponding to a 49 times improvement for electrical SNR. Considering the measured bandwidths for both cases, the calculated $\delta\nu_B$ for a 10 ns

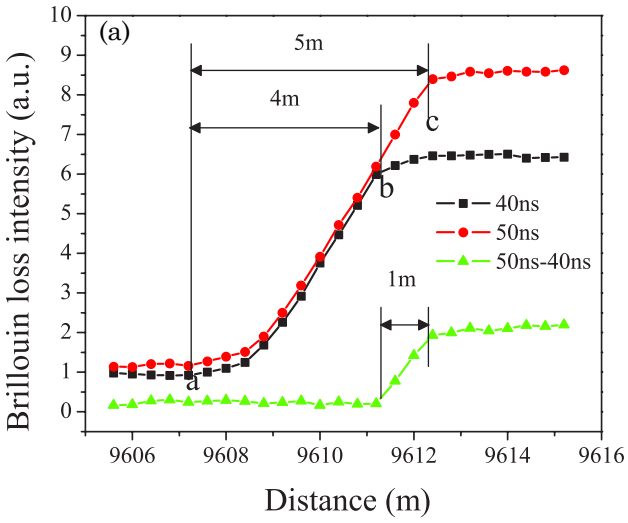

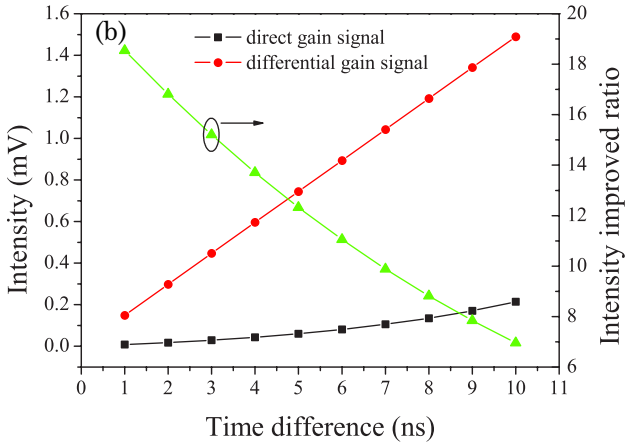

Fig. 3. (Color online) (a) Brillouin loss signals of the transition region for 40 ns and 50 ns pulses and their differential signal at the frequency difference of 10910 MHz. (b) Comparison of the direct gain signal and the differential gain signal.

pulse is 2.1 MHz, corresponding to a temperature uncertainty of 1.8 °C.

We also further study the temperature uncertainty with a pulse width of less than 10 ns for BOTDA and DPP-BOTDA. We consider a rectangular-shaped probe pulse with pulse width from 1 ns to 9 ns, with which the BGS bandwidth can be obtained by use of Eqs. (1) and (2). Taking into account the intensity improved ratio for direct and differential gain signals from Fig. 3(b), the calculated temperature uncertainty using Eq. (3) for BOTDA and DPP-BOTDA is shown in Fig. 5. For BOTDA, as pulse width decreases, the BGS bandwidth increases inversely proportional to the pulse width [9] and the Brillouin gain decreases exponentially, which results in a prompt increase of temperature uncertainty. It is as large as 90 °C for a 1 ns pulse. In fact, under this circumstance, the signal may be totally buried in the noise. So generally the pulse used in BOTDA is larger than 10 ns to obtain an adequate temperature accuracy for a sensing length of 10 km or larger. For

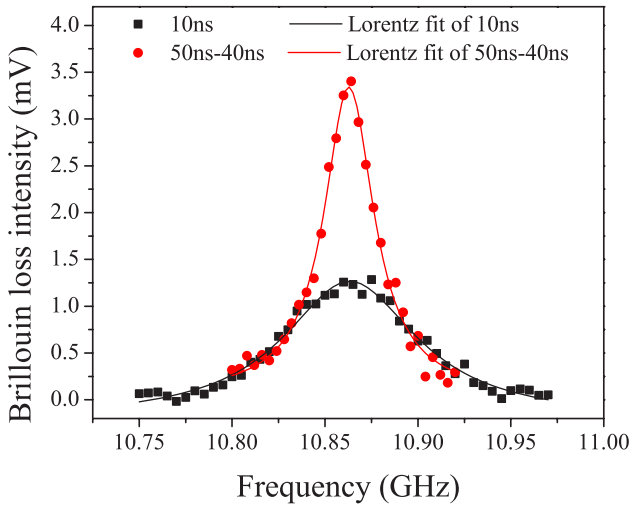

Fig. 4. (Color online) Measured BGSs for a 10 ns pulse and a 50/40 ns differential pulse pair.

DPP-BOTDA, as pulse-width difference decreases, the BGS bandwidth remains constant, and the differential gain just decreases linearly. The temperature uncertainty increases slight from 0.25 °C to 0.8 °C for DPP-BOTDA with spatial resolution from 1 m to 10 cm.

4. Summary

The trade-off between the spatial resolution and the BFS accuracy prohibits a conventional BOTDA system from obtaining a high spatial resolution and a high BFS accuracy simultaneously for sensing length of >10 km. For DPP-BOTDA, the differential Brillouin gain of two long pulses is much larger than the direct Brillouin gain of BOTDA and a narrowband BGS can be obtained, which provides an opportunity for centimeter spatial resolution with a high temperature accuracy. In this work we demonstrated a 12 km DPP-BOTDA using a 40/50 ns pulse pair with DC-coupled detection obtaining a spatial resolution of 1 m and a narrowband BGS of 33 MHz

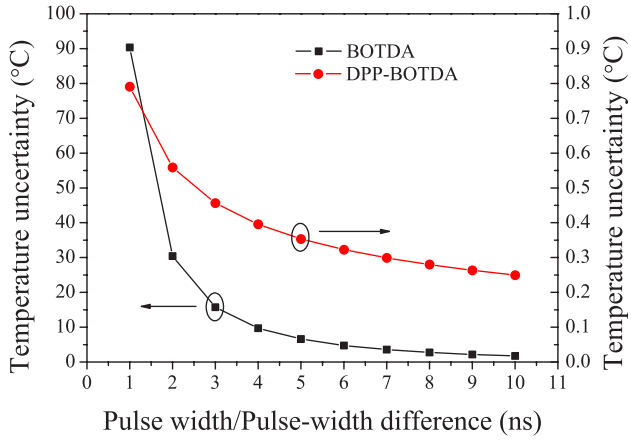

Fig. 5. (Color online) Comparison of the temperature uncertainty for BOTDA and DPP-BOTDA.

simultaneously, and temperature uncertainty for 40/50 ns pulses is improved to 0.25 °C compared with 1.8 °C for a 10 ns pulse. The calculation results also show that the temperature uncertainty is just increased to 0.8 °C for DPP-BOTDA at 1 ns pulse-width difference, which provides 10 cm spatial resolution.

This work is supported by the Natural Science and Engineering Research Council of Canada via the Discovery Grant and Canada Research Chair Program.

References

1. S. M. Maughan, H. H. Kee, and T. P. Newson, "57 km single-ended spontaneous Brillouin-based distributed fiber temperature sensor using microwave coherent detection," Opt. Lett. **26**, 331–333 (2001).
2. K. Shimizu, T. Horiguchi, Y. Koyamada, and T. Kurashima, "Coherent self-heterodyne detection of spontaneously Brillouin-scattered light waves in a single-mode fiber," Opt. Lett. **18**, 185–187 (1993).
3. X. Bao, D. J. Webb, and D. A. Jackon, "22 km distributed temperature sensor using Brillouin gain in an optical fiber," Opt. Lett. **18**, 552–554 (1993).
4. M. Nikles, L. Thevenaz, and P. A. Robert, "Simple distributed fiber sensor based on Brillouin gain spectrum analysis," Opt. Lett. **21**, 758–760 (1996).
5. W. Li, X. Bao, Y. Li, and L. Chen, "Differential pulse-width pair BOTDA for high spatial resolution sensing," Opt. Express **16**, 21616–21625 (2008).
6. X. Bao, Q. Yu, V. P. Kalosha, and L. Chen, "Influence of transient phonon relaxation on the Brillouin loss spectrum of nanosecond pulses," Opt. Lett. **31**, 888–890 (2006).
7. C. Zhang, W. Li, X. Bao, L. Chen, and M. Du, "Tensile strain dependence of the Brillouin gain spectrum in carbon/polyimide coated fibers," Opt. Lett. **32**, 2565–2567 (2007).
8. T. Horiguchi, K. Shimizu, and T. Kurashima, "Development of a distributed sensing technique using Brillouin scattering," J. Lightwave Technol. **13**, 1296–1302 (1995).
9. H. Naruse and M. Tateda, "Trade-off between the spatial and the frequency resolutions in measuring the power spectrum of the Brillouin backscattered light in an optical fiber," Appl. Opt. **38**, 6516–6521 (1999).